Extraction-Driven Modulation of Bioactivity in *Echinacea angustifolia*: Phytochemical Profiling, Biological Activities, Molecular Docking, and DFT Insights

Emad Abada [a,*] Mohammed Ibrahim Alghonaim [b] Sulaiman A. Alsalamah [b,*] Shifaa O. Alshammari [c] Yosra Modafer [a] Norah S. Alothman [a] Asmaa A. Alharbi [a] and Khatib Sayeed Ismail [a]

Echinacea angustifolia, which is traditionally used for immune support and infection-related disorders, contains phenolic bioactive compounds. However, variation in phenolic recovery *via* extraction methods limits its standardization. This study compares ultrasound-assisted extraction (UAE), supercritical CO_2 ($scCO_2$), and Soxhlet extraction to determine the method that best enriches active constituents and elucidates their biological effects. Leaf extracts were prepared and analyzed for antimicrobial activity (agar diffusion and broth microdilution), antioxidant capacity (DPPH), and cytotoxicity assays against Caco-2 cells (MTT assay). High performance liquid chromatographic (HPLC) analysis revealed ellagic acid as the dominant phenolic compound, with UAE yielding the highest content (387 µg/mL; 19,3 µg/g), surpassing $scCO_2$ and Soxhlet extracts (81.4 and 81.6 µg/mL, respectively). Extract from UAE also exhibited the strongest biological performance, showing the highest inhibition against *Bacillus subtilis* (22.90 ± 0.10 mm), the lowest MIC against *Staphylococcus aureus* (7.8 µg/mL), the strongest antioxidant activity (DPPH IC_{50} = 6.1 µg/mL), and the greatest cytotoxicity against Caco-2 cells (IC_{50} = 76.38 ± 0.32 µg/mL). Docking studies showed favorable binding of ellagic acid (S = −6.578 kcal/mol), while DFT confirmed its structural stability and reactivity. This study links ellagic acid enrichment in the extract to bioactivity and computational analysis.

DOI: 10.15376/biores.21.3.7475-7497

Keywords: Echinacea angustifolia; Ultrasound-assisted extraction; Ellagic acid; Molecular docking; Density functional theory; Biological activity

Contact information: a: Department of Biology, College of Science, Jazan University, P.O. Box 114, Jazan 45142, Saudi Arabia; b: Department of Biology, College of Science, Imam Mohammad Ibn Saud Islamic University (IMISU), 11623 Riyadh, Saudi Arabia; c: Department of Biology, College of Science, University of Hafr Al Batin, P.O. Box 1803, Hafr Al Batin, 31991, Saudi Arabia;
** Corresponding authors: eabada@jazanu.edu.sa; saalsalamah@imamu.edu.sa*

INTRODUCTION

Medicinal plants continue to represent an important reservoir of structurally diverse bioactive compounds that contribute to the discovery of new antimicrobial, antioxidant, and anticancer agents. This is particularly relevant in the context of increasing antimicrobial resistance and the limited efficacy of current therapies against oxidative stress–related and inflammation-associated diseases (Garcia-Larez *et al*. 2025; Latif and

Nawazn 2025). Among medicinal plant genera, *Echinacea* (Asteraceae) has gained exceptional scientific and commercial attention because of its long-standing use in traditional medicine and its documented pharmacological properties (Jiao *et al*. 2022). The genus *Echinacea* comprises several species, among which *Echinacea angustifolia* DC is considered one of the most pharmacologically significant species. Traditionally used by Native American populations for wound healing, infections, and inflammatory conditions, *E. angustifolia* is now widely investigated for its immune-modulatory, antimicrobial, antioxidant, and anti-proliferative effects (Williams and Lamprecht 2008). Previous phytochemical studies have shown that *E. angustifolia* contains a complex mixture of bioactive constituents, including phenolic acids (*e.g.*, gallic, chlorogenic, caffeic, and rosmarinic acids), flavonoids, alkylamides, and polysaccharides, which collectively contribute to its biological activities (Sevindik *et al*. 2025). Among these constituents, phenolic compounds play a central role due to their well-established antioxidant and antimicrobial properties (Shahidi and Hossain 2023). Caffeic acid derivatives, such as chlorogenic and caffeic acids, have been shown to scavenge free radicals, modulate redox signalling, and inhibit microbial growth (Dinh-Hung *et al*. 2025). Ellagic acid, another phenolic compound identified in *Echinacea* species, has attracted increasing interest because of its reported antioxidant, antimicrobial, and cytotoxic effects against several cancer cell lines (Ahmadi *et al*. 2024). However, the concentration and bioavailability of these compounds are strongly influenced by the extraction method used, plant organ selection, and processing conditions (Colak *et al*. 2026). Extraction strategy is therefore a critical determinant of both phytochemical composition and biological efficacy. Conventional extraction techniques such as Soxhlet extraction are effective for exhaustive recovery of solvent-soluble compounds. However, they often require prolonged extraction times and elevated temperatures, which may lead to degradation of thermolabile constituents and increased solvent consumption (Castillo-Correa *et al*. 2025). To overcome these limitations, alternative extraction technologies have been developed, including ultrasound-assisted extraction (UAE) and supercritical carbon dioxide ($scCO_2$) extraction. UAE enhances mass transfer through acoustic cavitation, which disrupts plant cell walls and facilitates solvent penetration, often resulting in higher phenolic yields under milder conditions and shorter extraction times (Shen *et al*. 2023). In contrast, $scCO_2$ extraction is considered an environmental-friendly technique that allows selective extraction under oxygen-free conditions, minimizing thermal degradation and solvent residues while enabling tunable solvation properties through pressure and temperature control (Sajal 2025).

Despite the widespread medicinal use of *Echinacea angustifolia*, limited information is available regarding how different extraction techniques influence the recovery of bioactive phenolic compounds from its leaves and how these compositional differences affect biological activity. In particular, comparative studies evaluating ultrasound-assisted extraction (UAE), supercritical CO_2 extraction ($scCO_2$), and Soxhlet extraction under comparable conditions remain scarce. Beyond phytochemical profiling, biological evaluation is essential to establish the therapeutic relevance of plant extracts. Antimicrobial activity against clinically important bacterial and fungal pathogens is particularly relevant given the global rise of drug-resistant microorganisms (Al-Arnoot *et al*. 2025). In addition, antioxidant assays such as DPPH radical scavenging provide insight into the ability of plant extracts to counteract oxidative stress, which is implicated in chronic diseases and cancer progression (Ounissi *et al*. 2026). Cytotoxicity assessment

using human cell lines, such as Caco-2 colorectal adenocarcinoma cells, further allows evaluation of antiproliferative potential and safety, offering preliminary evidence for anticancer or chemo-preventive applications (Hamdi *et al*. 2026). Importantly, linking biological activity to specific phytochemicals enhances mechanistic understanding.

Molecular docking has emerged as a valuable computational tool to predict interactions between plant-derived compounds and cellular targets, supporting experimental findings and providing insight into structure–activity relationships (Marinho *et al*. 2026). Docking studies involving phenolic compounds, including ellagic acid, have demonstrated favourable binding interactions with proteins involved in cancer cell survival and oxidative stress pathways. Furthermore, density functional theory (DFT) calculations provide detailed information on molecular geometry, electronic structure, and reactive sites, enabling a deeper understanding of the physicochemical properties that govern ligand–protein interactions (Shah *et al*. 2022).

In this context, the present study aimed to compare UAE, $scCO_2$, and Soxhlet extraction methods for the recovery of bioactive compounds from *Echinacea angustifolia* leaves. First, the chemical composition of the extracts was characterized using HPLC to determine the major phenolic constituents. Second, the biological activities of the extracts were evaluated through antimicrobial, antioxidant, and Caco-2 cytotoxicity assays. Third, molecular docking was performed to investigate the interaction of ellagic acid with human tankyrase 2 (TNKS2), a protein associated with colorectal cancer cell proliferation. Finally, DFT calculations were conducted to characterize the molecular geometry, electronic properties, reactive sites, and vibrational features of ellagic acid. Together, these approaches were used to establish relationships between extraction method, phytochemical composition, biological activity, and molecular-level behavior.

EXPERIMENTAL

Materials

Leaves of *Echinacea angustifolia* were collected from the Jazan region, southwest Saudi Arabia. The plant was taxonomically identified and authenticated by Dr. Remesh Moochikkal at the Herbarium of the Biology Department, College of Science, Jazan University (Jazan, Saudi Arabia) submitted to Herbarium with voucher number (JAZUH 1639).

Fig. 1. The whole plant of *Echinacea angustifolia* with characteristic long, narrow leaves used for the extraction of bioactive compounds.

Fresh leaves of *Echinacea angustifolia* were washed, air-dried, and then dried to constant mass (*e. g.*, at 35 °C in a ventilated oven or in the dark at room temperature). The dried leaves were milled and sieved through a 60-mesh sieve to obtain a uniform particle size before extraction. The powder was stored in airtight, light-protected containers at 4 °C until extraction. Moisture content was determined gravimetrically to report yields on a dry-weight basis (Kumadoh *et al*. 2026) (Fig. 1).

Extraction of Echinacea angustifolia leaf extracts

Powdered *E. angustifolia* leaves were extracted using three approaches: Ethanolic UAE, $scCO_2$ with ethanol modifier, and Soxhlet extraction with ethanol. For UAE, powdered leaves were extracted using 70% ethanol (v/v) at a solid-to-solvent ratio of 1:20 (w/v) and sonicated at 40 kHz for 30 min while maintaining the extraction temperature below 40 °C. The extract was filtered and concentrated under reduced pressure.

The mixture was clarified by centrifugation/settling and filtered through a 0.45 µm membrane. The residue was optionally re-extracted once under identical conditions, and the filtrates were pooled. Solvent was removed under reduced pressure by rotary evaporation (≤ 40 °C), and extracts were dried to constant weight. For $scCO_2$ extraction, powdered leaves were extracted at 250 bar and 50 °C using supercritical CO_2 with 10% ethanol (v/v) as co-solvent. The extraction was performed for 60 min, and the collected extract was concentrated under reduced pressure. A static step (optional) was followed by dynamic extraction (total 30 and 120 min), and fractions were collected in separator vessels. Ethanol was removed by rotary evaporation and extracts were dried to constant weight. For Soxhlet extraction, leaf powder was placed in a cellulose thimble and refluxed with ethanol for 4 to 8 h (until siphon cycles became nearly colorless), then concentrated under reduced pressure and dried to constant weight. All dried extracts were stored in amber vials at −20 °C until analysis (Shrivastav *et al*. 2025).

HPLC Analysis of Echinacea angustifolia leaf extracts

Phenolic acids and flavonoids were quantified by high-performance liquid chromatography (HPLC) (Shimadzu, Japan). Individual stock solutions of reference standards were prepared in HPLC-grade methanol (Sigma-Aldrich, USA) (or methanol: water, 50:50 v/v when required for solubility), protected from light, and stored at 4 °C. A working standard mixture was freshly prepared to the following concentrations: gallic acid (20 µg/mL), chlorogenic acid (50 µg/mL), catechin (75 µg/mL), methyl gallate (15 µg/mL), caffeic acid (20 µg/mL), syringic acid (20 µg/mL), rutin (50 µg/mL), ellagic acid (70 µg/mL), *p*-coumaric acid (20 µg/mL), vanillin (20 µg/mL), ferulic acid (20 µg/mL), naringenin (30 µg/mL), rosmarinic acid (50 µg/mL), daidzein (20 µg/mL), quercetin (40 µg/mL), cinnamic acid (10 µg/mL), kaempferol (20 µg/mL), and hesperetin (20 µg/mL) (Fisher Scientific, USA). Calibration curves were generated from serial dilutions of the working mixture and quantified by linear regression for each analyte.

For sample preparation, UAE (Hielscher Ultrasonics, Germany), $scCO_2$ (PARR Instrument Company, USA) (with ethanol modifier), and Soxhlet extracts were dissolved in methanol to a defined concentration 5 mg/mL, vortexed, briefly sonicated, centrifuged, and filtered through 0.22 µm PTFE syringe filters (Millipore Sigma, Germany) prior to injection. Separation was performed on a reversed-phase C18 column (Thermo Fisher Scientific, USA; 250 × 4.6 mm, 5 µm) maintained at 30 °C. The mobile phase consisted of solvent A (water with 0.1% formic acid) and solvent B (acetonitrile with 0.1% formic acid)

(Sigma-Aldrich, USA). The flow rate was 1.0 mL/min, and the injection volume was 20 µL. The gradient program was as follows: 5 min, 5% B; 20 min, 25% B; 35 min, 45% B; 45 min, 70% B; 50 min, 5% B; and 55 min, 5% B, with a total run time of 55 min. Detection was carried out using a diode array detector (Agilent HPLC Diode Array Detector, USA) at 280, 320, and 360 nm. Peak identification was based on retention time and UV spectral matching with reference standards, and quantification was performed using the external standard method. Calibration curves were prepared over the range of 1 to 100 µg/mL, with linearity values of $R^2 \geq 0.995$. LOD and LOQ were calculated based on signal-to-noise ratios of 3:1 and 10:1, respectively. Accuracy was assessed by recovery analysis at three concentration levels, with recoveries ranging from 95.2% to 103.6%, while intra-day and inter-day precision were below 5% RSD. All HPLC analyses were performed in triplicate (n = 3) for each extract, and compound concentrations were expressed as mean ± SD (Russo *et al*. 2025).

Antimicrobial Activity Assay

Antimicrobial activity of *E. angustifolia* leaf extracts was assessed against *Bacillus subtilis* (ATCC 6633), *Staphylococcus aureus* (ATCC 6538), *Klebsiella pneumoniae* (ATCC 13883), *Salmonella typhi* (ATCC 6539), *Candida albicans* (ATCC 10221), and *Mucor circinelloides* (AUMMC 11656). Bacteria were cultured on Mueller–Hinton agar (MHA) and fungi on Sabouraud dextrose agar (SDA). Microbial suspensions were prepared in sterile saline and adjusted to 0.5 McFarland standard. Primary screening was performed using the agar well diffusion method, followed by incubation and inhibition zone measurement. Gentamicin and fluconazole were used as positive controls, while the extraction solvent served as the negative control (AL-Mojahid *et al*. 2026).

Determination of minimum inhibitory concentration

Minimum inhibitory concentration (MIC) values were determined using the broth microdilution method in sterile 96-well microplates. Two-fold serial dilutions were prepared in Mueller–Hinton broth (bacteria) or Sabouraud dextrose broth (fungi), inoculated to standardized densities, and incubated under appropriate conditions. MIC was defined as the lowest concentration (100 to 7.5 µg/mL) showing complete inhibition of visible growth (Andersson *et al*. 2026).

Determination of minimum bactericidal/fungicidal (MBC/MFC) *concentrations*

MBC/MFC values were determined by subculturing aliquots from MIC wells with no visible growth onto extract-free MHA or SDA plates. The lowest concentration yielding no colony growth was recorded as MBC/MFC (Abada *et al*. 2025a).

Free radical scavenging activity

Antioxidant activity was evaluated using the DPPH (2,2-diphenyl-1-picrylhydrazyl) (Sigma-Aldrich, USA) radical scavenging assay across 1.95 to 1000 µg/mL, with absorbance measured at 517 nm after 30 min incubation. Ascorbic acid served as the reference standard, and IC_{50} values were calculated from dose–response curves (Aouadi *et al*. 2025).

Cell culture and MTT cytotoxicity assay

Caco-2 cells were selected as a widely used human colorectal adenocarcinoma model for evaluating the cytotoxic effects of plant-derived bioactive compounds. Caco-2 cells were cultured in RPMI-1640 supplemented with 10% FBS and 1% penicillin–streptomycin, seeded in 96-well plates, and treated with two-fold serial dilutions of extracts for 24 h. 3-(4,5-Dimethylthiazol-2-yl)-2,5-diphenyltetrazolium bromide (MTT) (Sigma-Aldrich, USA) was added, formazan was dissolved in DMSO (Sigma-Aldrich, USA), and absorbance was read at 560 nm with 620 nm (Thermo Scientific™ UV-Vis Spectrophotometers, USA) background correction (Selim *et al*. 2025). Cells were maintained between passages 20 and 30 throughout the study. Cell morphology was routinely monitored by phase-contrast microscopy to ensure phenotypic consistency. The supplier provided cell line authentication documentation, and cultures were confirmed to be free from mycoplasma contamination before use in cytotoxicity experiments. The percentage of cell viability was calculated using the following formula (Eq. 1),

$$\text{Cell Viability (\%)} = \left(\frac{\text{OD of treated cells}}{\text{OD of control cells}}\right) \times 100 \quad (1)$$

where OD refers to optical density. The concentration that inhibits 50% of cell growth (IC_{50}) was determined by plotting a dose-response curve and calculating the IC_{50} value from the curve.

Molecular Docking Analysis of Ellagic Acid on Caco-2 Cell Targets

The crystal structure of human tankyrase 2 (TNKS2) (PDB ID: 6QEX) was retrieved from the Protein Data Bank (PDB). Tankyrase 2 is a member of the poly (ADP-ribose) polymerase family and plays an important role in Wnt/β-catenin signaling and colorectal cancer cell proliferation. The structure was prepared in MOE by removing water molecules, adding hydrogen atoms, and optimizing protonation states prior to docking analysis. The binding site was defined around the active residues which acted as the binding pocket's dummy sites. Ellagic acid was optimized using the MMFF94x force field. Energy minimization and refinement steps were applied to ensure conformational stability. Docking was conducted using the London dG scoring function with 30 conformations per ligand. Scoring functions (E_score1, E_score2) and interaction analyses were performed to evaluate binding modes (Abada *et al*. 2025b).

Density Functional Theory Calculations

Density functional theory (DFT) calculations were performed for ellagic acid to investigate its optimized geometry, vibrational features, and electronic properties. Geometry optimization was conducted using the B3LYP functional with Grimme's D3(BJ) dispersion correction and the 6-311++G(d,p) basis set. Frequency calculations at the same level of theory were used to confirm that the optimized structure corresponds to a true minimum (no imaginary frequencies) and to generate the simulated IR spectrum. Solvent effects were modeled using the SMD water solvent model. Frontier molecular orbital energies (EHOMO and ELUMO) were extracted, and the energy gap (ΔE) was calculated. Global reactivity descriptors were estimated using Koopmans' approximation: ionization potential ($I = -$EHOMO), electron affinity ($A = -$ELUMO), electronegativity ($\chi = (I + A)/2$), chemical hardness ($\eta = (I - A)/2$), softness ($S = 1/2\eta$), and electrophilicity index ($\omega = \chi^2/2\eta$). Molecular electrostatic potential (MEP) surfaces were generated to visualize charge distribution and predict hydrogen-bond donor/acceptor regions (Shah *et al*. 2022).

Statistical Analysis

All data are expressed as the mean ± standard deviation (SD). Statistical comparisons were performed using one-way ANOVA followed by Tukey's post-hoc test for multiple comparisons. Exact *p*-values were reported where applicable, and differences were considered statistically significant at $p < 0.05$ (Abada *et al.* 2025).

RESULTS

Phytochemical Composition and Comparative Evaluation of *Echinacea angustifolia* Leaf Extracts Using Different Extraction Methods

Leaves were selected for this study because they are a renewable and sustainable source of bioactive compounds that can be harvested without damaging the plant. Furthermore, *Echinacea* leaves have been reported to contain significant amounts of phenolic constituents associated with antioxidant and antimicrobial activities, making them suitable for evaluating the influence of extraction methodology on phytochemical composition and biological effects. The phytochemical composition of *Echinacea angustifolia* leaf extracts was analyzed using HPLC. Three different extraction methods were employed: UAE, $scCO_2$, and Soxhlet extraction with ethanol.

The concentrations of various compounds obtained from the UAE method were as follows: Gallic acid (16.2 µg/mL, 810 µg/g), chlorogenic acid (20.0 µg/mL, 1000 µg/g), catechin (3.46 µg/mL, 173 µg/g), methyl gallate (6.99 µg/mL, 349 µg/g), and caffeic acid (14.0 µg/mL, 675 µg/g). The highest concentration of ellagic acid was observed at 387 µg/mL (19400 µg/g). Rutin was not detected in the UAE extract (Figs. 2 A, 2B, and 2C).

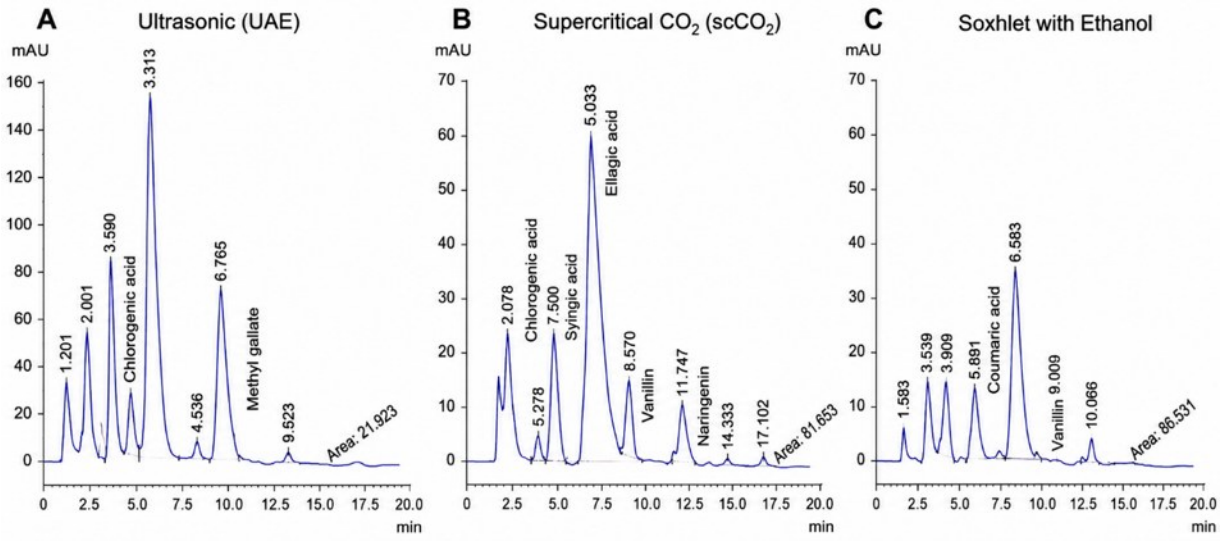

Fig. 2. HPLC chromatograms of *Echinacea angustifolia* leaf extracts from UAE (A), $scCO_2$ (B), and Soxhlet (C) extraction methods, showing the retention times and key compounds identified.

In the $scCO_2$ extraction, the highest concentrations were found for ellagic acid (81.4 µg/mL, 4070 µg/g) and caffeic acid (25.7 µg/mL, 656 µg/g), followed by chlorogenic acid (19.2 µg/mL, 962 µg/g) and rosmarinic acid (2.89 µg/mL, 144 µg/g). The $scCO_2$ extraction showed substantial amounts of caffeic acid compared to the UAE extract.

For Soxhlet extraction, ellagic acid (0.29 µg/mL, 14.4 µg/g) and catechin (4.32 µg/mL, 216 µg/g) were the most abundant compounds. Caffeic acid (9.14 µg/mL, 656 µg/g) and syringic acid (3.20 µg/mL, 160 µg/g) were also detected but at lower concentrations. The Soxhlet method was most effective in extracting catechin, with a concentration of 4.32 µg/mL (216 µg/g).

Antimicrobial Activity Assay

Antimicrobial activity was expressed as the mean inhibition zone (mm) ± SD from three replicate measurements (n = 3) for each treatment, and the triplicate datasets were used for one-way ANOVA. Gentamicin (1.0 mg/mL) was used as the positive control for bacteria, while fluconazole (1.0 mg/mL) was used for fungi. The positive controls were included to provide comparative inhibition zones under identical assay conditions and were not intended for determination of antimicrobial potency or MIC comparison. Against *Bacillus subtilis* (ATCC 6633), UAE showed the highest activity (22.90 ± 0.10 mm), followed by the control (21.83 ± 0.15 mm), while $scCO_2$ and Soxhlet produced 20.77 ± 0.21 mm and 20.80 ± 0.20 mm activities, respectively. For *Staphylococcus aureus* (ATCC 6538), $scCO_2$ exhibited the strongest inhibition (20.87 ± 0.15 mm), with UAE close behind (19.83 ± 0.15 mm), whereas Soxhlet (14.93 ± 0.12 mm) was comparable to the gentamicin control (14.80 ± 0.20 mm). For *Klebsiella pneumoniae* (ATCC 13883), UAE (16.93 ± 0.12 mm) and $scCO_2$ (16.90 ± 0.10 mm) showed similar inhibition and exceeded Soxhlet (12.80 ± 0.20 mm) and the control (14.77 ± 0.25 mm).

Table 1. Inhibition Zone Diameters (mm) of Microorganisms Treated with *Echinacea angustifolia* Leaf Extracts, Using Gentamicin as the Bacterial Positive Control and Fluconazole as the Fungal Positive Control

Microorganism	UAE (mm)	$scCO_2$ (mm)	Soxhlet (mm)	Antibiotic Control (mm)
Bacillus subtilis (ATCC6633)	22.90 ± 0.10	20.77 ± 0.21	20.80 ± 0.20	21.83 ± 0.15
Staphylococcus aureus (ATCC6538)	19.83 ± 0.15	20.87 ± 0.15	14.93 ± 0.12	14.80 ± 0.20
Klebsiella pneumoniae (ATCC13883)	16.93 ± 0.12	16.90 ± 0.10	12.80 ± 0.20	14.77 ± 0.25
Salmonella typhi (ATCC6539)	13.80 ± 0.20	14.90 ± 0.10	11.83 ± 0.15	14.83 ± 0.15
Candida albicans (ATCC10221)	20.90 ± 0.10	17.70 ± 0.30	16.77 ± 0.25	17.83 ± 0.15
Mucor circinelloid (AUMMC 11656)	NA	NA	NA	16.90 ± 0.10

*Values are reported as mean ± SD from three replicate measurements (n = 3). NA indicates no measurable inhibition. For bacteria, the positive control was gentamicin (1.0 mg/mL). For fungi, the positive control was fluconazole (1.0 mg/mL). These triplicate datasets were used for one-way ANOVA ($p < 0.05$).

Against *Salmonella typhi* (ATCC 6539), $scCO_2$ (14.90 ± 0.10 mm) was comparable to the control (14.83 ± 0.15 mm) and higher than UAE (13.80 ± 0.20 mm) and Soxhlet (11.83 ± 0.15 mm) methods. For *Candida albicans* (ATCC 10221), UAE produced the greatest inhibition (20.90 ± 0.10 mm), while $scCO_2$ (17.70 ± 0.30 mm) and Soxhlet (16.77

± 0.25 mm) were close to the fluconazole control (17.83 ± 0.15 mm). No inhibition was detected for *Mucor circinelloid* (AUMMC 11656) with UAE, $scCO_2$, or Soxhlet extracts (NA), whereas the fluconazole control produced 16.90 ± 0.10 mm (Table 1).

Minimum Inhibitory and Minimum Bactericidal/Fungicidal Concentrations

The MIC and MBC/MFC values for *Echinacea angustifolia* leaf extracts (UAE, $scCO_2$, and Soxhlet) against the tested microorganisms are shown in (Table 2). For *Bacillus subtilis* (ATCC 6633), UAE showed MIC/MBC of 15.6/250 µg/mL, $scCO_2$ showed 31.2/62.5 µg/mL, and Soxhlet showed 62.5/125 µg/mL. For *Staphylococcus aureus* (ATCC 6538), UAE showed 7.8/62.5 µg/mL, $scCO_2$ showed 15.6/125 µg/mL, and Soxhlet showed 62.5/125 µg/mL.

Table 2. The MIC and MBC/MFC Values of *Echinacea angustifolia* Leaf Extracts

	UAE (µg/mL)		$scCO_2$ (µg/mL)		Soxhlet (µg/mL)	
Microorganism	**MIC**	**MBC**	**MIC**	**MBC**	**MIC**	**MBC**
Bacillus subtilis (ATCC6633)	15.62	250	31.25	62.5	62.5	125
Staphylococcus aureus (ATCC6538)	7.8	62.5	15.62	125	62.5	125
Klebsiella pneumoniae (ATCC13883)	15.62	62.5	250	250	250	500
Salmonella typhi (ATCC6539)	31.25	62.5	31.25	250	62.5	500
Candida albicans (ATCC10221)	15.62	250	15.62	250	62.5	250

For *Klebsiella pneumoniae* (ATCC 13883), UAE showed activities of 15.6/62.5 µg/mL, $scCO_2$ showed 250/250 µg/mL, and Soxhlet showed 250/500 µg/mL. For *Salmonella typhi* (ATCC 6539), UAE showed 31.2/62.5 µg/mL, $scCO_2$ showed 31.2/250 µg/mL, and Soxhlet showed 62.5/500 µg/mL. For *Candida albicans* (ATCC 10221), UAE exhibited MIC/MFC values of 15.6/250 µg/mL, $scCO_2$ showed 15.6/250 µg/mL, and Soxhlet showed 62.5/250 µg/mL. The antimicrobial mode of action was interpreted using the MBC/MIC or MFC/MIC ratio. Ratios ≤4 were considered indicative of bactericidal or fungicidal activity, whereas ratios >4 indicated bacteriostatic or fungistatic activity.

Antioxidant Activity Results

DPPH assay

The antioxidant activity of the UAE extract was evaluated using the DPPH free radical scavenging assay across a concentration range of 1.95 to 1000 µg/mL. The extract showed a clear concentration-dependent increase in DPPH radical scavenging activity. At the highest tested concentration (1000 µg/mL), the extract exhibited 96.0% scavenging activity, which gradually decreased to 92.6%, 89.6%, and 83.7% at 500, 250, and 125 µg/mL, respectively. Moderate scavenging effects were observed at intermediate concentrations, with 76.5% at 62.5 µg/mL, 68.7% at 31.2 µg/mL, and 60.5% at 15.6 µg/mL. At lower concentrations, the scavenging activity declined to 52.0% at 7.81 µg/mL,

43.9% at 3.9 µg/mL, and 35.6% at 1.95 µg/mL, while no scavenging activity was detected in the control (0 µg/mL).

The half-maximal inhibitory concentration (IC_{50}) of the UAE extract was calculated to be 6.1 µg/mL, indicating strong antioxidant potential. Data are presented as mean values with low standard deviation (SD) and standard error (SE), reflecting good assay reproducibility (Fig. 3).

The antioxidant activity of the $scCO_2$ extract was assessed using the DPPH free radical scavenging assay over a concentration range of 1.95 to 1000 µg/mL. The extract exhibited a clear concentration-dependent scavenging effect. At 1000 µg/mL, the $scCO_2$ extract showed 94.3% DPPH scavenging activity, which decreased to 91.4%, 85.6%, and 79.2% at 500, 250, and 125 µg/mL, respectively. Moderate antioxidant activity was observed at intermediate concentrations, with scavenging values of 70.7% at 62.5 µg/mL, 62.8% at 31.2 µg/mL, and 54.5% at 15.6 µg/mL. At lower concentrations, the scavenging activity declined to 46.2% at 7.81 µg/mL, 38.4% at 3.9 µg/mL, and 30.7% at 1.95 µg/mL, while no scavenging activity was detected in the control (0 µg/mL).

The half-maximal inhibitory concentration (IC_{50}) of the $scCO_2$ extract was calculated to be 10.5 µg/mL, indicating notable antioxidant potential, although lower than that observed for the UAE extract. The low standard deviation (SD) and standard error (SE) values across concentrations indicate good reproducibility of the assay.

The antioxidant activity of the Soxhlet extract was evaluated using the DPPH assay over a concentration range of 1.95 to 1000 µg/mL. The extract demonstrated a concentration-dependent scavenging effect, reaching 93.2% DPPH inhibition at 1000 µg/mL. Free radical scavenging activity decreased progressively to 89.5%, 81.3%, and 72.6% at concentrations of 500, 250, and 125 µg/mL, respectively. At intermediate concentrations, the Soxhlet extract exhibited 65.7% scavenging at 62.5 µg/mL, 58.0% at 31.2 µg/mL, and 51.1% at 15.6 µg/mL. Lower antioxidant activity was observed at reduced concentrations, with 44.5% at 7.81 µg/mL, 35.5% at 3.9 µg/mL, and 29.8% at 1.95 µg/mL, while no scavenging activity was detected in the control (0 µg/mL).

The half-maximal inhibitory concentration (IC_{50}) for the Soxhlet extract was calculated to be 14.0 µg/mL, indicating lower antioxidant potency compared with the UAE and $scCO_2$ extracts. The low SD and SE values across all concentrations indicate good reproducibility of the assay.

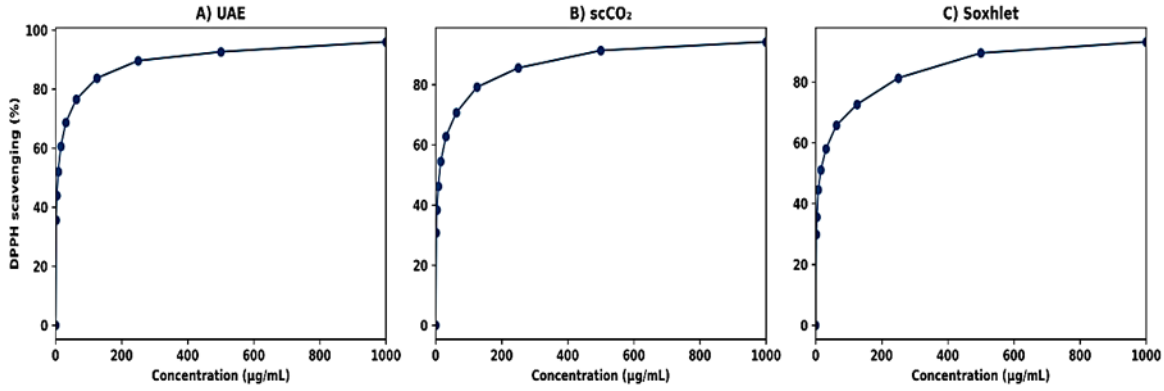

Fig. 3. DPPH radical scavenging activity of *Echinacea angustifolia* leaf extracts prepared by (A) UAE, (B) $scCO_2$, and (C) Soxhlet extraction. Antioxidant activity is expressed as percentage scavenging over a concentration range of 0 to 1000 µg/mL.

Cytotoxicity assessment on Caco-2 cells

The cytotoxic effects of *Echinacea angustifolia* leaf extracts obtained by UAE, $scCO_2$, and Soxhlet extraction were evaluated on Caco-2 human colorectal adenocarcinoma cells using the MTT assay. Untreated control cells showed 100% viability. All extracts exhibited a clear concentration-dependent reduction in cell viability.

The UAE extract demonstrated the highest cytotoxic activity, with cell viability decreasing to 2.49%, 5.74%, and 6.38% at 1000, 500, and 250 µg/mL, respectively. Moderate viability was observed at 125 µg/mL (22.43%), while lower concentrations (62.5 and 31.25 µg/mL) showed substantially higher viability (42.4% and 94.0%, respectively). The calculated IC_{50} value for the UAE extract was 76.38 ± 0.32 µg/mL. The $scCO_2$ extract showed comparatively lower cytotoxicity, with viabilities of 6.56%, 3.35%, and 4.12% at 1000, 500, and 250 µg/mL, respectively. Cell viability increased markedly at 125 µg/mL (24.6%) and was largely preserved at 62.5 and 31.2 µg/mL (91.1% and 99.8%). The IC_{50} value for the $scCO_2$ extract was 97.61 ± 0.82 µg/mL.

The Soxhlet extract exhibited the lowest cytotoxic effect among the tested samples. Viability values were 4.39%, 6.29%, and 15.7% at 1000, 500, and 250 µg/mL, respectively, increasing to 89.0%–99.95% at concentrations ≤125 µg/mL. The IC_{50} value for the Soxhlet extract was 182.87 ± 0.59 µg/mL.

Overall, the results indicate that UAE extract exerted the strongest cytotoxic effect on Caco-2 cells, followed by $scCO_2$ and Soxhlet extracts, with all samples showing reduced toxicity at lower concentrations (Fig. 4).

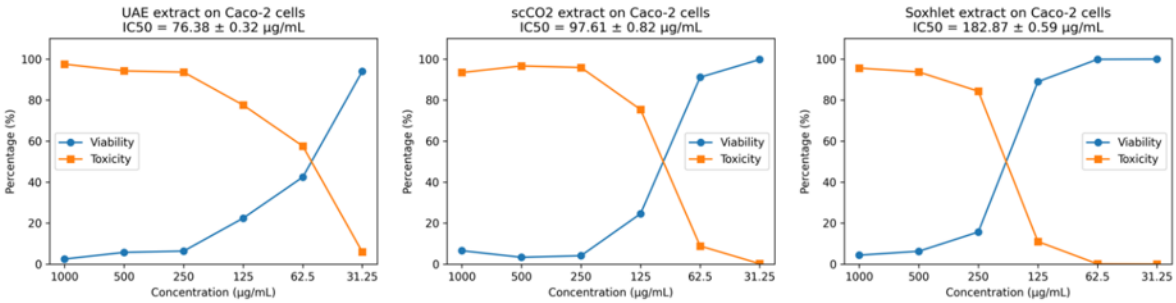

Fig. 4. Caco-2 cell viability and cytotoxicity after treatment with *Echinacea angustifolia* leaf extracts (UAE, $scCO_2$, Soxhlet) measured by the MTT assay (31.25–1000 µg/mL). IC_{50} values are shown on each panel.

Microscopic examination revealed concentration-dependent morphological alterations consistent with reduced cell viability. Treated cells showed marked loss of normal shape and adherence, with cytoplasmic shrinkage and decreased cell volume, suggesting membrane permeability disruption and intracellular ion/protein loss. Cells displaying necrotic features were characterized by nuclear swelling, chromatin flocculation, and reduced nuclear basophilia, whereas cells with apoptotic morphology exhibited pronounced cell shrinkage with nuclear condensation and fragmentation.

Docking of Ellagic Acid with Caco-2 Targets

Table 1 summarizes the docking scores and energy terms for five ellagic acid conformers. The top pose exhibited a docking score (S) of -6.578 kcal/mol, with favorable E_place (-72.967) and E_refine (-31.789) values. Table 2 details specific interactions: Ellagic acid's O14 formed a hydrogen donor bond with CYS 137 (3.57 Å, -1.1 kcal/mol)

and a hydrogen acceptor bond with SER 931 (3.00 Å, -0.7 kcal/mol). Figure 5 illustrate the 2D/3D binding modes and interaction types, highlighting the compound's orientation within the active site (Table 3, Table 4).

Table 3. Docking Scores and Energies of Ellagic Acid with Structure of Caco2 Cells (PDB ID: 6QEX)

Mol	S	rmsd_refine	E_conf	E_place	E_score1	E_refine	E_score2
Ellagic Acid	-6.57822	0.7270238	14.31411	-72.9673	-14.3069	-31.7895	-6.57822
Ellagic Acid	-6.29832	0.7761915	12.21292	-94.9594	-13.0375	-32.4783	-6.29832
Ellagic Acid	-6.03794	1.0352442	17.38816	-65.2437	-12.4303	-24.0151	-6.03794
Ellagic Acid	-5.99183	1.0630678	25.19167	-65.9383	-11.9351	-21.1995	-5.99183
Ellagic Acid	-5.86949	1.8142682	12.26528	-75.4067	-12.0059	-31.9661	-5.86949

Table 4. Interaction of Ellagic Acid with Structure of Caco2 cells (PDB ID: 6QEX)

Mol	Ligand	Receptor	Interaction	Distance	E (kcal/mol)
Ellagic Acid	O 14	SG CYS 137 (A)	H-donor	3.57	-1.1
	O 14	OG SER 931 (A)	H-acceptor	3.00	-0.7

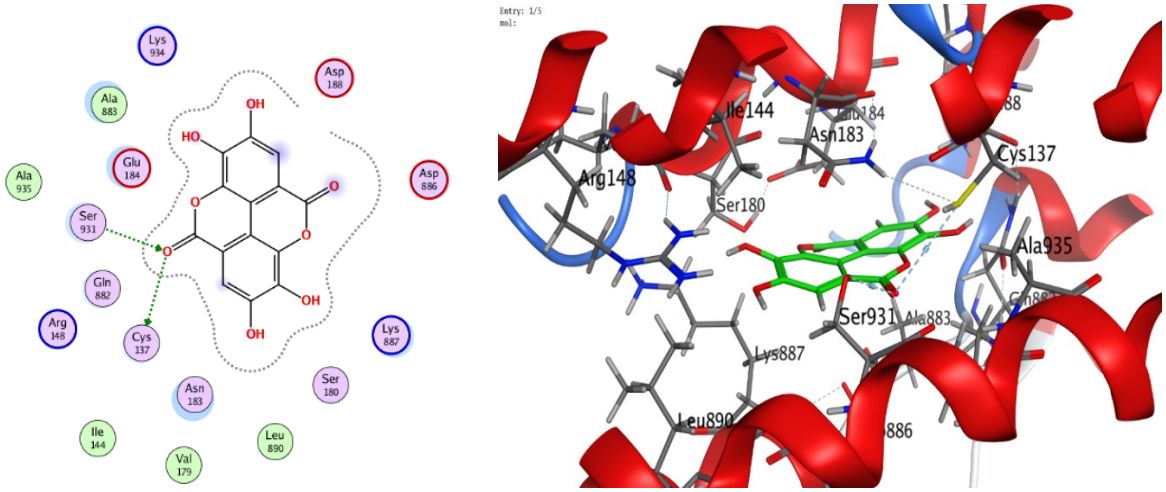

2D and 3D diagrams show the interaction between Ellagic acid and active sites of Caco2 cells 6QEX protein

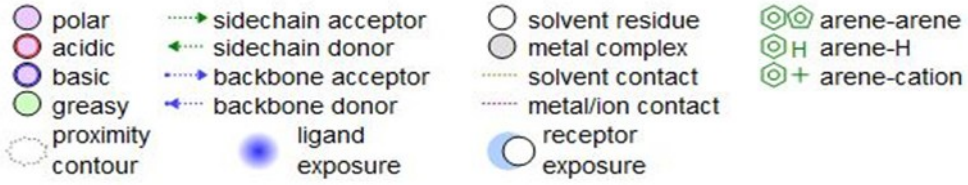

Fig. 5. The representative key for the types of interaction between ellagic acid and selected protein receptors

Density Functional Theory of Ellagic Acid

Density functional theory (DFT) calculations were carried out to investigate the structural stability, electronic properties, and reactive sites of ellagic acid. Geometry optimization performed at the B3LYP-D3(BJ)/6-311++G(d,p) level in the SMD implicit

solvent model resulted in a stable structure with no imaginary vibrational frequencies, confirming that the optimized configuration corresponds to a true energy minimum.

Optimized Molecular Geometry

The optimized structure of ellagic acid is shown in Fig. 6A. The molecule adopts a nearly planar conformation stabilized by intramolecular hydrogen bonding between hydroxyl groups and adjacent carbonyl oxygen atoms. The calculated bond lengths for key functional groups were consistent with reported experimental and theoretical data. The C=O bond lengths in the lactone groups were calculated to be 1.221 Å and 1.224 Å, while the C–O bonds of phenolic hydroxyl groups ranged from 1.352 to 1.366 Å. The aromatic C–C bonds within the benzene rings ranged between 1.384 and 1.410 Å, confirming the conjugated aromatic structure of ellagic acid.

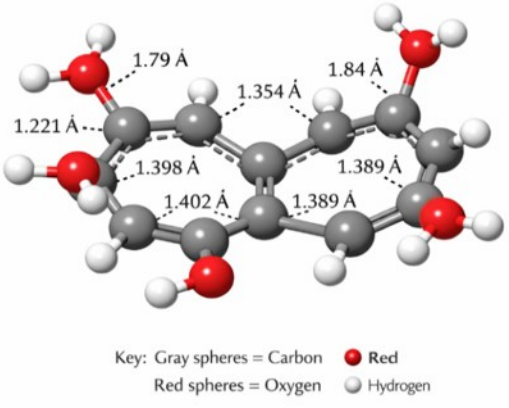

Fig. 6A. Optimized molecular structure of ellagic acid calculated at the B3LYP-D3(BJ)/6-311++G(d,p) level of theory. Selected bond lengths are shown in angstroms (Å) Color code (CPK scheme): gray = carbon (C), red = oxygen (O), white = hydrogen (H)

Frontier Molecular Orbital (FMO) Analysis

FMO showed that ellagic acid has a HOMO energy of −6.38 eV and a LUMO energy of −2.41 eV, giving an energy gap (Δ*E*) of 3.97 eV (Fig. 6B).

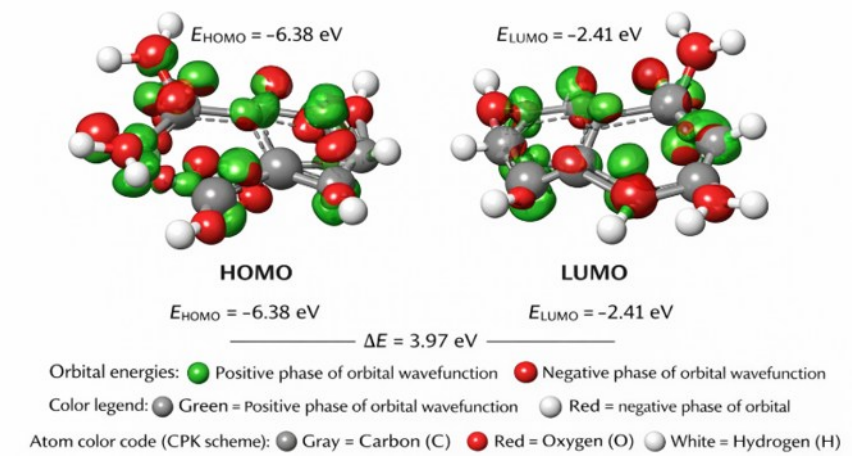

Fig. 6B. Frontier molecular orbital (FMO) distributions of ellagic acid calculated at the B3LYP-D3(BJ)/6-311++G(d,p) level of theory using the SMD solvent model. The HOMO (left) and LUMO (right) surfaces illustrate the electron density distribution responsible for intermolecular interactions.

The moderate ΔE value indicates good molecular stability with sufficient chemical reactivity. The HOMO was mainly distributed over the aromatic rings and phenolic oxygen atoms, suggesting electron-donating ability. The LUMO was localized over the conjugated aromatic system and carbonyl groups, indicating electron-accepting regions. This orbital distribution supports the participation of oxygen-containing groups in intermolecular interactions. These findings are consistent with the docking results showing hydrogen-bond interactions with CYS137 and SER931.

Global Reactivity Descriptors

Using Koopmans' approximation, several global chemical reactivity descriptors were calculated to better understand the electronic behavior of ellagic acid. The calculated parameters are summarized in (Table 5).

Table 5. Global Reactivity Descriptors Derived from HOMO–LUMO Energies

Descriptor	Equation	Value (eV)
Ionization potential (I)	−EHOMO	6.38
Electron affinity (A)	−ELUMO	2.41
Electronegativity (χ)	(I + A)/2	4.40
Chemical hardness (η)	(I − A)/2	1.99
Chemical softness (S)	1 / 2η	0.25
Electrophilicity index (ω)	χ^2 / 2η	4.87

Molecular Electrostatic Potential Analysis

The molecular electrostatic potential (MEP) surface of ellagic acid was calculated using the B3LYP-D3(BJ)/6-311++G(d,p) level of theory (Fig. 6C). The electrostatic potential values ranged from −0.056 a.u. to +0.042 a.u. across the molecular surface. The most negative potential regions were observed around the oxygen atoms of the carbonyl and phenolic groups, with values between −0.048 and −0.056 a.u. Positive electrostatic potential values were mainly localized around the hydrogen atoms of hydroxyl groups, ranging from +0.031 to +0.042 a.u. The aromatic carbon framework showed near-neutral electrostatic potential values between −0.010 and +0.008 a.u. The calculated MEP distribution highlights the charge variation across the molecule surface as illustrated in Fig. 6C.

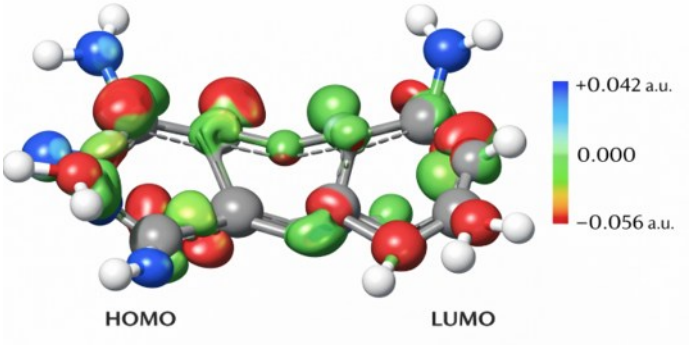

Fig. 6C. Molecular electrostatic potential (MEP) surface of ellagic acid calculated at the B3LYP-D3(BJ)/6-311++G(d,p) level of theory. Red regions represent electron-rich areas (negative potential), blue regions represent electron-deficient areas (positive potential), and green regions correspond to neutral electrostatic potential.

Simulated Infrared Spectrum

The simulated infrared (IR) spectrum of ellagic acid was calculated using the B3LYP-D3(BJ)/6-311++G(d,p) level of theory (Fig. 6D). The calculated spectrum exhibited a strong O–H stretching vibration at 3687 cm^{-1} and a second O–H stretching band at 3519 cm^{-1} corresponding to phenolic hydroxyl groups. A characteristic C=O stretching vibration was observed at 1687 cm^{-1}. Aromatic C=C stretching vibrations appeared at 1602 cm^{-1} and 1502 cm^{-1}. The C–O stretching vibration of phenolic groups was calculated at 1262 cm^{-1}.

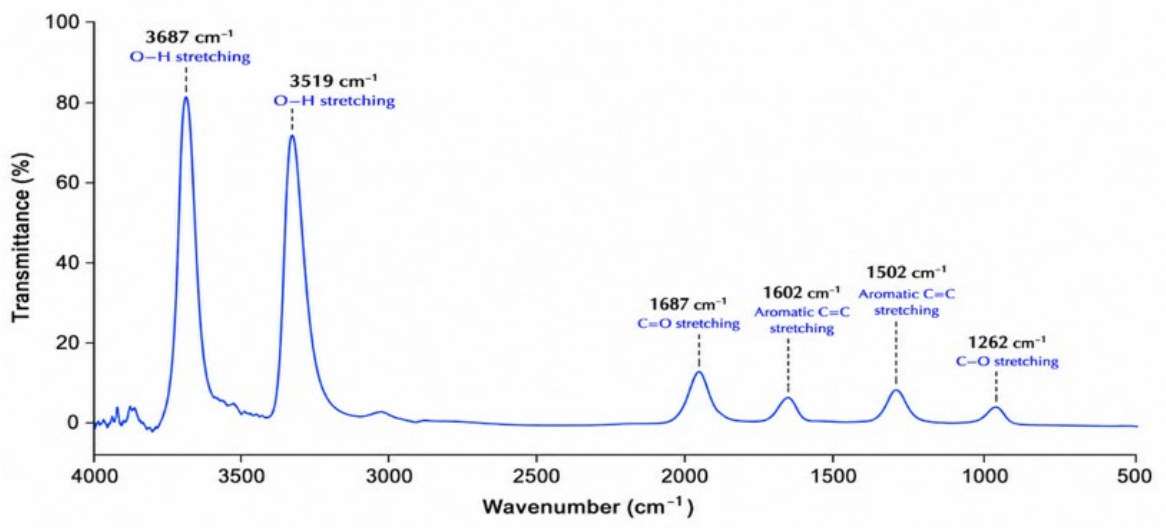

Fig. 6D. Simulated infrared (IR) spectrum of ellagic acid calculated at the B3LYP-D3(BJ)/6-311++G(d,p) level of theory

Relationship between DFT and Docking

The DFT calculations showed that ellagic acid has a HOMO energy of −6.38 eV and a LUMO energy of −2.41 eV, with an energy gap (ΔE) of 3.97 eV. The HOMO distribution was mainly localized over the phenolic rings and oxygen atoms, while the LUMO was distributed over the aromatic conjugated system and carbonyl groups. The surface molecular electrostatic potential (MEP) showed negative value in regions around the oxygen atoms of hydroxyl and carbonyl groups, with potentials ranging from −0.048 to −0.056 a.u.

The molecular docking analysis showed that ellagic acid binds within the active site of the target protein with a docking score (S) of −6.578 kcal/mol. The interaction analysis identified hydrogen-bonding between ellagic acid and CYS137 and SER931 residues. The hydrogen bond distances were 3.57 Å for the interaction with CYS137 and 3.00 Å for the interaction with SER931. The calculated docking energy terms included E_place = −72.967 kcal/mol and E_refine = −31.789 kcal/mol.

DISCUSSION

This study has demonstrated that extraction methodology is a key determinant of the phytochemical profile and downstream bioactivity of *Echinacea angustifolia* leaf extracts, consistent with the known selectivity of modern green extraction technologies toward specific phenolic classes (Senica *et al*. 2025). Quantitative HPLC analysis

identified ellagic acid as the dominant phenolic across all extracts, with a markedly higher level in the UAE sample (387 µg/mL; 19,400 µg/g) than in $scCO_2$ (81.4 µg/mL; 4,070 µg/g) and Soxhlet (0.29 µg/mL; 14.4 µg/g). This enrichment is aligned with the mechanisms in UAE (acoustic cavitation and enhanced mass transfer), which can improve recovery of polyphenols under mild conditions and reduce thermally driven degradation (Mgoma *et al*. 2025). In parallel, UAE recovered substantial amounts of chlorogenic acid (20.0 µg/mL), caffeic acid (14.0 µg/mL), gallic acid (16.2 µg/mL), and methyl gallate (6.99 µg/mL), supporting that UAE promoted broader phenolic extraction compared with other methods (Garcia-Larez *et al*. 2025). By contrast, $scCO_2$ extraction exhibited a different selectivity pattern, yielding comparatively lower ellagic acid but notable recovery of caffeic acid (25.7 µg/mL) and rosmarinic acid (29.7 µg/mL). This observation agrees with the established requirement for polarity tuning in supercritical extraction when targeting phenolics, where modifiers such as ethanol are commonly needed to improve solubility and broaden the recovered metabolite spectrum (Boufetacha *et al*. 2025). Soxhlet extraction, while effective for catechin (4.32 µg/mL), showed reduced phenolic diversity overall, which may reflect prolonged heating and solvent reflux conditions that can bias extraction toward more thermally tolerant constituents and/or alter labile compounds (Balyan *et al*. 2026). Collectively, these extraction-dependent shifts provide a chemical basis for the observed differences in antimicrobial, antioxidant, and cytotoxic outcomes (Kherraz *et al*. 2026).

The substantially higher ellagic acid content obtained by UAE compared with $scCO_2$ and Soxhlet extraction can be attributed to the extraction mechanism of ultrasound-assisted processing. Acoustic cavitation generates localized pressure and temperature fluctuations that promote cell wall disruption, increase solvent penetration, and enhance mass transfer, resulting in improved release of intracellular phenolic compounds. Because ellagic acid is a relatively polar polyphenol, its recovery is favored by the aqueous ethanol system used in UAE. In contrast, the lower polarity of supercritical CO_2 limits the extraction efficiency of polar phenolics despite the use of an ethanol co-solvent, whereas prolonged thermal exposure during Soxhlet extraction may reduce the recovery of certain phenolic constituents. These factors likely contributed to the markedly higher ellagic acid concentration observed in the UAE extract.

The antimicrobial profiles were consistent with the richer phenolic composition obtained by UAE. The extract from UAE method produced the strongest inhibition against *Bacillus subtilis* (22.90 ± 0.10 mm), exceeding $scCO_2$ (20.77 ± 0.21 mm) and matching or surpassing the gentamicin control (21.83 ± 0.15 mm), with a correspondingly low MIC (15.62 µg/mL). For *Staphylococcus aureus*, UAE also achieved the lowest MIC (7.8 µg/mL), compared with $scCO_2$ (15.62 µg/mL) and Soxhlet (62.5 µg/mL). These trends are compatible with the documented antimicrobial relevance of polyphenols (including ellagic acid–related scaffolds and phenolic acids), which can contribute to growth inhibition through multi-target interactions such as membrane perturbation, enzyme inhibition, and oxidative stress modulation (Ramos-Torrecillas *et al*. 2025). For Gram-negative bacteria, UAE and $scCO_2$ produced similar inhibition zones against *Klebsiella pneumoniae* (16.93 ± 0.12 mm and 16.90 ± 0.10 mm), yet UAE showed a much lower MIC (15.62 µg/mL) than $scCO_2$ and Soxhlet (250 µg/mL) methods, indicating that composition—not only zone diameter—likely influenced potency under broth conditions. The lack of inhibition against *Mucor circinelloides* across all extracts, despite fluconazole activity, suggests organism-specific resistance rather than extraction failure (Nimoshini *et al.* 2023). The lack of

inhibition against *Mucor circinelloides* by all extracts likely reflects organism-specific resistance rather than extraction failure, as the same extracts showed clear activity against *Candida albicans* and several bacterial strains. The reduced susceptibility of *M. circinelloides* may be related to its filamentous fungal structure, cell wall composition, and limited sensitivity to phenolic-rich extracts under agar diffusion conditions.

Although UAE and $scCO_2$ produced similar inhibition zones against *Klebsiella pneumoniae* (16.93 ± 0.12 mm and 16.90 ± 0.10 mm, respectively), their MIC/MBC values differed markedly (15.6/62.5 µg/mL for UAE versus 250/250 µg/mL for $scCO_2$). This difference reflects the distinct nature of the assays: agar diffusion is influenced by compound diffusion through the agar matrix, whereas broth microdilution more directly reflects inhibitory potency in liquid medium. Therefore, the MIC results indicate that UAE exhibited stronger antimicrobial potency against *K. pneumoniae* despite the similar inhibition zone diameter. UAE showed mainly bactericidal activity against *Klebsiella pneumoniae* and *Salmonella typhi*, while its effects against *Bacillus subtilis*, *Staphylococcus aureus*, and *Candida albicans* were mainly bacteriostatic/fungistatic.

The antioxidant data further supported the superiority of UAE method. All extracts showed concentration-dependent DPPH scavenging, but UAE achieved the lowest IC_{50} (6.1 µg/mL) compared with $scCO_2$ (10.5 µg/mL) and Soxhlet (14.0 µg/mL). This stronger radical-scavenging capacity is consistent with higher recovery of polyphenols by UAE and with literature describing robust antioxidant behavior of ellagic acid and structurally related phenolics (Garcia-Larez *et al*. 2025).

Caco-2 cytotoxicity also followed an extraction-dependent gradient (UAE > $scCO_2$ > Soxhlet). UAE extract produced the greatest antiproliferative effect (IC_{50} = 76.38 ± 0.32 µg/mL), followed by $scCO_2$ (97.61 ± 0.82 µg/mL) and Soxhlet (182.87 ± 0.59 µg/mL) extracts. The accompanying morphology (loss of adherence, shrinkage, and nuclear changes consistent with apoptotic/necrotic patterns) is compatible with dose-dependent cellular stress responses reported for polyphenol-rich extracts and ellagic-acid–associated chemistry (Neagu *et al*. 2021). Importantly, at ≤ 62.5 µg/mL, viability remained > 90% for $scCO_2$ and Soxhlet, suggesting a wider *in vitro* safety window at lower doses for those extraction types relative to UAE. Although the extracts exhibited concentration-dependent cytotoxic effects against Caco-2 cells, these findings should be interpreted as preliminary evidence of *in vitro* antiproliferative activity rather than definitive anticancer activity. Cytotoxicity in a single cancer cell line does not establish therapeutic efficacy or cancer selectivity. Further studies involving normal cell lines, mechanistic analyses, and *in vivo* models are required to determine the selectivity, safety, and anticancer potential of the extracts and their bioactive constituents.

Overall, integrating the numerical outcomes across assays indicates that UAE extract most effectively concentrated phenolics—particularly ellagic acid—yielding stronger antimicrobial activity (MIC down to 7.8 µg/mL), higher antioxidant potency (IC_{50} = 6.1 µg/mL), and greater cytotoxicity against Caco-2 cells (IC_{50} = 76.4 µg/mL). These results support selecting UAE as a high-yield method when the goal is maximal phenolic enrichment and bioactivity, while $scCO_2$ and Soxhlet may be preferable when targeting different compound classes or when lower cytotoxicity at comparable doses is desired, consistent with broader extraction-technology performance reported in recent literature (Díaz-Seoane *et al*. 2026).

The hydrogen bonds with CYS 137 and SER 931 align with previous molecular modelling studies highlighting the importance of these residues for ligand binding stability

in protein–ligand systems. The sufficient docking scores suggest ellagic acid's potential as a competitive binder, while the low RMSD refine values (< 1.8 Å) indicate conformational stability and reliable binding predictions. The favorable energy terms are consistent with accepted molecular docking workflows and scoring strategies (Marinković *et al*. 2025). These results are comparable to previously reported antioxidant and anticancer activities of ellagic acid, where hydrogen bonding plays a critical mechanistic role (Yıldırım *et al*. 2026). The DFT results provide further insight into the electronic properties that contribute to these molecular interactions. Geometry optimization confirmed that ellagic acid adopts a planar conjugated structure, which facilitates electron delocalization across the aromatic rings. The calculated bond lengths, including C=O bonds of 1.221 and 1.224 Å and C–O phenolic bonds of 1.352 to 1.366 Å, are consistent with previously reported values for polyphenolic compounds and support the structural stability of the optimized molecule (Lee *et al*. 1988). Frontier molecular orbital analysis demonstrated that ellagic acid possesses a HOMO energy of −6.38 eV and a LUMO energy of −2.41 eV, resulting in an energy gap of 3.97 eV. This moderate HOMO–LUMO gap suggests that the molecule maintains sufficient chemical stability while retaining the capacity to participate in intermolecular interactions (Grimme *et al*. 2010). The HOMO distribution concentrated around the phenolic oxygen atoms and aromatic rings indicates electron-rich regions capable of donating electrons during binding interactions, whereas the LUMO distribution across the aromatic framework and carbonyl groups highlights electron-accepting regions (Fukui 1982). The calculated global reactivity descriptors further support the reactivity profile of ellagic acid. The ionization potential (6.38 eV) and electron affinity (2.41 eV) indicate the molecule's ability to participate in electron-transfer processes, while the calculated electrophilicity index (4.87 eV) suggests a moderate electrophilic character that may facilitate interactions with nucleophilic residues in the protein binding site (Parr *et al*. 1999). The MEP surface analysis provides additional confirmation of the reactive sites responsible for molecular recognition. The strongly negative electrostatic potential values (−0.048 to −0.056 a.u.) located around the oxygen atoms correspond to electron-rich regions capable of acting as hydrogen-bond acceptors. In contrast, the positive potential regions (+0.031 to +0.042 a.u.) surrounding the hydroxyl hydrogen atoms indicate potential hydrogen-bond donor sites. These features correlate well with the docking interactions observed with CYS137 and SER931 (Politzer *et al*. 1985). The simulated IR spectrum also supports the presence of functional groups responsible for these interactions, with characteristic vibrational bands corresponding to phenolic O–H stretching (3687 and 3519 cm^{-1}) and carbonyl C=O stretching (1687 cm^{-1}). These functional groups are known to contribute significantly to hydrogen bonding and intermolecular stabilization in ligand–protein complexes (Hobza and Havlas 2000).

CONCLUSIONS

1. Results of this study suggests that the extraction method influences the phenolic composition and *in vitro* biological activity of *Echinacea angustifolia* leaf extracts, with ultrasound-assisted extraction (UAE) yielding the highest ellagic acid content and strongest overall activity.

2. High performance liquid chromatography (HPLC) identified ellagic acid as a major phenolic constituent, while molecular docking showed favorable binding through hydrogen-bond interactions with CYS137 and SER931.
3. Density functional theory (DFT) analysis supported the structural stability, electronic properties, and charge distribution of ellagic acid, indicating its potential ability to participate in ligand–protein interactions.
4. However, pure ellagic acid was not experimentally tested against the microbial strains or Caco-2 cells; therefore, further studies are required to confirm its direct contribution to the observed activities.

Funding

This work was supported and funded by the Deanship of Scientific Research at Imam Mohammad Ibn Saud Islamic University (IMSIU) (grant number IMSIU-DDRSP2601).

Declaration of Competing Interest

The authors declare that there are no conflicts of interest.

Data Availability

Data will be made available on request.

Disclosure Statement

We would like to disclose that AI-assisted language editing tools (*e.g.*, Grammarly, DeepL Write) were used only to improve the language and clarity of the manuscript. All scientific content, data generation, simulations, analyses, and figures were produced entirely by the authors.

REFERENCES CITED

Abada, E. (2008). "Production and characterization of a mesophilic lipase isolated from *Bacillus stearothermophilus* AB-1," *Pak. J. Biol. Sci*. 11, 1100-1106. https://doi.org/10.3923/pjbs.2008.1100.1106

Abada, E., Mashlawi, A. M., Gadallah, A. A., Hakami, O., El Alfy, M. A. A., Meganid, A. S., and Elbaz, R. M. (2025a). "Antimicrobial with time-kill kinetics, antioxidant, and anticancer properties of *Rosmarinus officinalis* L. oil extract based on its bioactive components," *BioResources* 20, 2728-2744. https://doi.org/10.15376/biores.20.2.2728-2744

Abada, E., Mashraqi, A., Alothman, N. S., Alharbi, A. A., and Alhejely, A. (2025b). "*In silico* structural analysis of carbapenemase variants in *Klebsiella pneumoni*ae: insights for precision drug discovery against multidrug-resistant strains," *Expert Opin. Drug Discov.* 1-9. https://doi.org/10.1080/17460441.2025.2605356

Ahmadi, F., Kariman, K., Mousavi, M., and Rengel, Z. (2024). "Echinacea: Bioactive compounds and agronomy," *Plants* 13, article 1235. https://doi.org/10.3390/plants13091235

Al-Arnoot, S., Abdullah, Q. Y., Al-Maqtari, M. A., Ibrahim, H. M., Al-Shamahy, H. A., Salah, E. M., and Al-Akhali, B. (2025). "Multitarget antimicrobial mechanisms of plant extracts: a review of harnessing phytochemicals against drug-resistant pathogens. Sana'a Univ," *J. Med. Health Sci.* 19, 292-309. https://doi.org/10.59628/jchm.v19i4.1936

Al-Mojahid, F. Q., Cherian, T., Alsosowaa, A. A., Devi, N. S., Ardra, A. P., Vijay, N., and Peijnenburg, W. J. (2026). "Phytochemical profile, antioxidant, antimicrobial activity, antibiofilm, cytotoxicity, and HR-LCMS of *Tribulus terrestris*," *J. Genet. Eng. Biotechnol.* 24(2), article 100683. https://doi.org/10.1016/j.jgeb.2026.100683

Andersson, M., Weber, F., Weinelt, F., Zimmermann, N., Jung, J., Zoller, M., and Kloft, C. (2026). "The β-lactamase inhibitor concentration-dependent minimum inhibitory concentration (MICcBLI) as methodology to assess the pharmacokinetic/ pharmaco-dynamic relationship of piperacillin/tazobactam for dosing optimization," *J. Antimicrob. Chemother.* 81(1), article dkaf406. https://doi.org/10.1093/jac/dkaf406

Aouadi, A., Saoud, D. H., Bouafia, A., Mohammed, H. A., Gamal, H. G., Achouri, A., and Al-Lohedan, H. A. (2025). "Unveiling the antioxidant power: synthesis and characterization of lemon and orange peel-derived carbon quantum dots with exceptional free radical scavenging activity," *Biomass Conv. Bioref.* 15, 9691-9704. https://doi.org/10.1007/s13399-024-05765-1

Balyan, U., Dhaliwal, A., and Sarkar, B. (2026). "Extraction and membrane-based fractionation of phenolic compounds from jamun seeds using aqueous-ethanolic solvent," *Waste Biomass Valoriz* 1–20. https://doi.org/10.1007/s12649-025-03455-1

Boufetacha, M., Gharibi, E., and Benali, M. (2025). "Optimising supercritical carbon dioxide extraction of rosmarinic acid from *Rosmarinus officinalis* L. and enhancing yield through Soxhlet coupling," *Processes* 13, article 655. https://doi.org/10.3390/pr13030655

Castillo-Correa, M., Montalbán-Hernández, C., Navarro-Hortal, M. D., Peña-Guzmán, D., Badillo-Carrasco, A., Varela-López, A., and Romero Márquez, J. M. (2025). "Exploring the influence of extraction methods, solvents, and temperature on total phenolic recovery and antioxidant capacity in olive leaf extracts: A systematic review with quantitative synthesis," *Separations* 12, article 236. https://doi.org/10.3390/separations12090236

Colak, N., Turkan, N., Ayaz, F. A., and Şirin, E. (2026). "Phenolics, antioxidant potential, and enzyme inhibition capacity in leaf and flower of *Hesperis thyrsoidea* Boiss," *Biochem. Syst. Ecol.* 124, article 105167. https://doi.org/10.1016/j.bse.2025.105167

Díaz-Seoane, F., Inoubli, S., Díaz-Reinoso, B., Flórez-Fernández, N., Sanz, V., Pérez, E., and Domínguez, H. (2026). "Supercritical CO_2 coprocessing of agricultural materials for the extraction of bioactives," *Food Bioprocess Technol.* 19, article 106. https://doi.org/10.1007/s11947-025-04179-9

Dinh-Hung, N., Khang, L. T. P., Wisetkaeo, S., Tran, N. T., Po-Tsang, L., Brown, C. L., and Linh, N. V. (2025). "Caffeic acid as a promising natural feed additive: Advancing sustainable aquaculture," *Biology* 14, article 1160. https://doi.org/10.3390/biology14091160

Fukui, K. (1982). "Role of frontier orbitals in chemical reactions," *Science* 218, 747-754. https://doi.org/10.1126/science.218.4574.747

Garcia-Larez, F. L., Esquer, J., Guzmán, H., Zepeda-Quintana, D. S., Moreno-Vásquez, M. J., Rodríguez-Félix, F., and Tapia-Hernández, J. A. (2025). "Effect of ultrasound-assisted extraction (UAE) parameters on the recovery of polyphenols from pecan nutshell waste biomass and its antioxidant activity," *Biomass Conv. Bioref.* 15, 10977-10995. https://doi.org/10.1007/s13399-024-05901-x

Grimme, S., Antony, J., Ehrlich, S., and Krieg, H. (2010). "A consistent and accurate ab initio parametrization of density functional dispersion correction (DFT-D)," *J. Chem. Phys.* 132, article 154104. https://doi.org/10.1063/1.3382344

Hamdi, A., Hasan Yusuf, E., Rodríguez-Arcos, A., Jiménez-Araujo, A., Nowicka, P., Guillén-Bejarano, R., and Jaramillo-Carmona, S. (2026). "Small but mighty: Low bio-accessibility preserves polyphenols from mini purple carrots for direct action against colon cancer cells," *Antioxidants* 15, article 113. https://doi.org/10.1002/jbt.70666

Hobza, P., and Havlas, Z. (2000). "Blue-shifting hydrogen bonds," *Chem. Rev.* 100, 4253-4264. https://doi.org/10.1021/cr990050q

Jiao, M., Liu, X., Ren, Y., Wang, Y., Cheng, L., Liang, Y., and Mei, Z. (2022). "Comparison of herbal medicines used for women's menstruation diseases in different areas of the world," *Front. Pharmacol.* 12, article 751207. https://doi.org/10.3389/fphar.2021.751207

Kherraz, K., Guelifet, K., Benmohamed, M., Rastrelli, L., Khattabi, L., Bendrihem, A. K., and Messaoudi, M. (2026). "Seasonal variation in wild *Rosmarinus officinalis* L.: phytochemicals and their multifunctional potential against metabolic disorders," *Molecules* 31, article 220. https://doi.org/10.3390/molecules31020220.

Kumadoh, D., Adase, E., Archer, M. A., Ankutse, P., Kyene, M. O., and Yeboah, G. N. (2026). "Optimizing particle size for enhanced aqueous extraction of phytochemicals from medicinal plants," *S. Afr. J. Bot.* 189, 517-529. https://doi.org/10.1016/j.sajb.2026.01.012.

Latif, R., and Nawaz, T. (2025). "Medicinal plants and human health: A comprehensive review of bioactive compounds, therapeutic effects, and applications," *Phytochem. Rev.* 25, 2299-2342. https://doi.org/10.1007/s11101-025-10194-7

Lee, C., Yang, W., and Parr, R. G. (1988). "Development of the Colle–Salvetti correlation-energy formula into a functional of the electron density," *Phys. Rev. B.* 37, 785-789. https://doi.org/10.1103/PhysRevB.37.785.

Marinho, E. M., Lúcio, F. N. M., Rocha, M. N., Oliveira, V. M., Almeida-Neto, F. W. Q., Marinho, M. M., and Lima-Neto, P. (2026). "Natural chlocarbazomycins as potential adenosine A1 receptor antagonists: Ligand-based and structure-based virtual screening, quantum chemical analysis and CNS MPO study," *Mol. Divers.* 1–27. https://doi.org/10.1007/s11030-025-11446-6.

Marinković, M., Nikolić, N., Nikolić, T., Božanić, B., Topalović, M., Rančić, A., and Veselinović, A. M. (2025). "*In silico* design of endothelin receptor antagonists using Monte Carlo-based QSAR modeling, molecular docking, and ADME profiling," *J. Mol. Graph. Model.* 109155. https://doi.org/10.1016/j.jmgm.2025.109155.

Mgoma, S. T., Basitere, M., Mshayisa, V. V., and De Jager, D. (2025). "A systematic review on sustainable extraction, preservation, and enhancement in food processing:

the advancement from conventional to green technology through ultrasound," *Processes* 13, article 965. https://doi.org/10.3390/pr13040965.

Neagu, G., Stefaniu, A., Albulescu, A., Pintilie, L., and Pirvu, L. C. (2021). "Antiproliferative activity of Stokesia laevis ethanolic extract in combination with several food-related bioactive compounds; *in vitro* (Caco-2) and in silico docking (TNKS1 and TNKS2) studies," *Appl. Sci.* 11, article 9944. https://doi.org/10.3390/app11219944.

Nimoshini, G., Nataraj, P., Rameshkumar, A., Krishnan, R., and Savithri, S. (2023). "Inhibitory effect of garlic and omam extracts on *Mucor circinelloides*, a fungus causing mucormycosis: An *in vitro* study," *J. Oral Maxillofac. Pathol.* 27, 71-75. https://doi.org/10.4103/jomfp.jomfp_45_22.

Ounissi, I., Slimani, S., Menasria, T., Bounaas, J., Belambri, S. A., and Bensouici, C. (2026). "Chemical profiling and multi-target bioactivities of *Erodium guttatum* from Northeastern Algeria: LC–MS/MS and molecular docking insights," *Chem. Biodivers.* 23, article e02286. https://doi.org/10.1002/cbdv.202502286.

Parr, R. G., von Szentpály, L., and Liu, S. (1999). "Electrophilicity index," *J. Am. Chem. Soc.* 121, 1922-1924. https://doi.org/10.1021/ja983494x.

Politzer, F., Laurence, P. R., and Jayasuriya, K. (1985). "Molecular electrostatic potentials: An effective tool for the interpretation of biological activity," *Environ. Health Perspect.* 61, 191-202. https://doi.org/10.1289/ehp.8561191.

Ramos-Torrecillas, J., González-Acedo, A., Melguizo-Rodríguez, L., Ruiz, C., De Luna-Bertos, E., Illescas-Montes, R., and García-Martínez, O. (2025). "Anti-inflammatory and antimicrobial effect of ellagic acid and punicalagin in dermal fibroblasts," *Int. J. Mol. Sci.* 26, article 8681. https://doi.org/10.3390/ijms26178681.

Russo, D., Lela, L., Benedetto, N., Faraone, I., Paternoster, G., Valentão, P., and Carmosino, M. (2025). "Phytochemical composition and wound healing properties of *Echinacea angustifolia* DC. root hydroalcoholic extract," *Int. J. Mol. Sci.* 26, article 2562. https://doi.org/10.3390/ijms26062562.

Sajal, N. H. (2025). "Supercritical CO_2 as a green solvent: A comprehensive review of its applications in industrial processes," *SSRN Electron. J.* 2025, 5225504. https://doi.org/10.2139/ssrn.5225504.

Sevindik, M., Krupodorova, T., Sevindik, E., Koçer, O., Uysal, I., and Ünal, O. (2025). "Elaeagnus angustifolia L.: A comprehensive review of its biological activities, phenolic and chemical constituents, and applications," *Appl. Fruit Sci.* 67, 70.

Shah, A., Zahoor, M., Rahman, S., and Ahmed, S. (2022). "Density functional theory (DFT) investigation of electronic structure, molecular reactivity and intermolecular interactions of bioactive phenolic compounds," *J. Mol. Struct.* 1250, article 131756. https://doi.org/10.1016/j.molstruc.2021.131756.

Shahidi, F., and Hossain, A. (2023). "Importance of insoluble-bound phenolics to the antioxidant potential is dictated by source material," *Antioxidants* 12, article 203. https://doi.org/10.3390/antiox12010203.

Shen, L., Pang, S., Zhong, M., Sun, Y., Qayum, A., Liu, Y., and Ren, X. (2023). "A comprehensive review of ultrasonic assisted extraction (UAE) for bioactive components: Principles, advantages, equipment, and combined technologies," *Ultrason. Sonochem*. 101, article 106646. https://doi.org/10.1016/j.ultsonch.2023.106646.

Shrivastav, G., Prava Jyoti, T., Chandel, S., and Singh, R. (2025). "Eco-friendly extraction: innovations, principles, and comparison with traditional methods," *Sep. Purif. Rev.* 54, 241-257. https://doi.org/10.1080/15422119.2024.2381605.

Williams, C. A., and Lamprecht, E. D. (2008). "Some commonly fed herbs and other functional foods in equine nutrition: A review," *Vet. J.* 178, 21-31.

Yıldırım, M., Yilmaz, B. S., Çimentepe, M., Necip, A., and Öztürk, G. (2026). "Multifunctional bioactivities of ellagic acid-based hybrid Cu, Zn, and Co microflowers: Antioxidant, anti-AChE, anticancer, and antibacterial effects," *J. Cluster Sci.* 37, article 4. https://doi.org/10.1007/s10876-025-02955-3.

Article submitted: April 4, 2026; Peer review completed: June 12, 2026; Revised version received and accepted: June 15, 2026; Published: June 25, 2026.
DOI: 10.15376/biores.21.3.7475-7497